Ferrichrome: Surprising Stability of a Cyclic Peptide–Fe^{III} Complex Revealed by Mass Spectrometry

Igor A. Kaltashov and Robert J. Cotter
Department of Pharmacology and Molecular Sciences, Johns Hopkins University School of Medicine, Baltimore, Maryland, USA

W. Harry Feinstone
University of Memphis, Memphis, Tennessee, USA

Gary W. Ketner
Department of Molecular Microbiology and Immunology, Johns Hopkins University School of Hygiene and Public Health, Baltimore, Maryland, USA

Amina S. Woods
Department of Oncology, Johns Hopkins University School of Medicine, Baltimore, Maryland, USA

Ferrichrome, a fungal siderophore that is also utilized by some bacterial species, was studied with liquid secondary ion mass spectrometry (LSIMS) and matrix-assisted laser desorption ionization (MALDI) mass spectrometry. A strong ionic signal corresponding to a Fe^{III} complex was observed with LSIMS in the positive ion mode. Switching the polarity of the mass spectrometer did not necessarily result in reduction of ferric ion, although certain conditions led to appearance of a Fe^{II} complex signal as well. The results of the structural studies of the metal ion-cyclic peptide complex with collisionally induced dissociation allowed unambiguous identification of the chelation sites. The action of the siderophore on Fe^{III} was studied by in vitro chelation of ferric ion (from ferric citrate) by the iron-free ferrichrome. Effective chelation of ferric ion was compared to actions of the iron-free ferrichrome on other metal ions. Unlike LSIMS, desorption with MALDI did not form selectively molecular ions of intact ferrichrome: the spectra contained abundant peaks corresponding to the cyclic peptide itself and its nonspecific association with alkali metal ions. (J Am Soc Mass Spectrom 1997, 8, 1070–1077) © 1997 American Society for Mass Spectrometry

Iron is a mineral essential for normal growth of a vast majority of microorganisms [1–3]. Under aerobic conditions the abundance of free iron is limited because of the very low solubility of ferric hydroxide. To maintain required levels of iron intracellularly, bacteria and fungi, as well as gramineous plants, elaborate effective ferric ion chelating agents, called siderophores, to scavenge for iron in the extracellular environment and transport it inside the microorganism [3, 4]. In recent years, siderophores began attracting growing interest in the medical community, inspired by hopes of employing them as effective delivery systems for antimicrobial agents [5].

Although siderophores can be easily isolated as iron chelates in large quantities, structural studies of the intact complexes are quite difficult to perform due to the high spin of the ferric ion that leads to broadening of ^1H NMR bands. Application of x-ray crystallography to structural characterization of siderophores has been also somewhat limited owing to the fact that less than a half of known siderophores can be crystallized [3, 6]. Another powerful analytical tool for structure characterization of siderophores via analysis of electronic state of iron ions in such compounds is Mössbauer spectroscopy [7]. Mass spectrometry has also been proven to be a valuable tool in siderophore structure elucidation, although earlier studies of iron-containing phytosiderophores by fast atom bombardment (FAB) mass spectrometry [8] revealed that a prompt reduction of Fe^{III} to Fe^{II} takes place inside the ion source. This promotes a change in the metal ion coordination geometry, rendering impossible a direct determination of chelation sites within the complex.

Ferrichrome, one of the first discovered sid-

Address reprint requests to Professor R.J. Cotter, Department of Pharmacology and Molecular Sciences, Johns Hopkins University School of Medicine, 725 N. Wolfe Street, Baltimore, MD 21205. E-mail: rcotter@welchlink.welch.jhu.edu

1044-0305/97/$17.00
PII S1044-0305(97)00128-1

Received March 10, 1997
Revised May 12, 1997
Accepted May 16, 1997

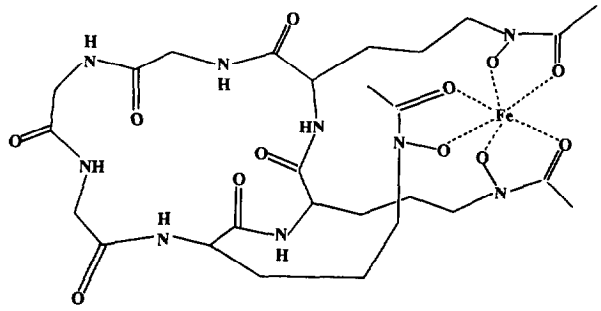

Figure 1. Chemical structure of ferrichrome [6].

erophores, was originally extracted from a rust fungus *Ustilago sphaerogena* [9]. It was found later that the very same siderophore, if present in the environment, can also be utilized by several bacterial species, including *E. coli* [3]. It is a cyclic peptide containing three glycine and three modified ornithine residues, with six oxygen atoms employed to chelate Fe^{III} (Figure 1). The Fe^{III} affinity of ferrichrome is very high, as suggested by a rather low reduction potential of the complex, $E_{1/2} < -0.6$ V at pH 8 [10]. Nevertheless, the binding of the metal ion to the cyclic peptide is reversible, and the complex dissociates nondestructively (i.e., release of the metal ion leaves the peptide intact) inside the fungal cell following the reduction of Fe^{III} to Fe^{II} [10]. We report here on the results of mass spectral studies of the structure of the metal-containing ferrichrome, that reveal a remarkable stability of the complex.

Experimental

Materials

The siderophore was obtained from a field isolate (A31) of *Aspergillus* tentatively identified as *A. flavofurcatus*. For production of the siderophore, A31 cultures were grown in minimal medium supplemented with yeast extract at 28–30 °C in a well aerated fermenter. Purification was by ion-exchange, reverse-phase, and gel filtration chromatography and will be described elsewhere. The siderophore is a potent inhibitor of growth of bacteriophages including T1 and ϕ80 [11], and a bacteriophage T1 growth-reduction bioassay was used to monitor purification steps. Iron-free ferrichrome (from *U. sphaerogena*), calcium acetate, zinc acetate, and ferric citrate were purchased from Sigma Chemical Co. (St. Louis, MO).

Mass Spectrometry. LSIMS spectra were acquired on a Concept IH (Kratos Analytical, Manchester, UK) two-sector (EB geometry) mass spectrometer at a resolution of 1000. A 1-μL aliquot of sample solution in water was mixed with the matrix (3-nitrobenzyl alcohol, 3-NBA or monothioglycerol, MTG) on the tip of the probe. Analyte ions were desorbed from the matrix by an 8-keV Cs^+ primary-ion beam. The mass spectra were acquired by scanning the magnet at a 10-s/decade scan rate. B/E linked scans were employed to acquire the spectra of the product ions following high-energy collision-induced dissociation (CID) (Xe, 50% attenuation) of the precursor ions in the first field-free region of the mass spectrometer. Normally 5–50 scans were averaged for each spectrum.

MALDI time-of-flight (TOF) mass spectra were acquired on Kompact III (dual-stage reflectron) and Kompact IV (curved-field reflectron) TOF mass spectrometers (Kratos Analytical, Manchester, UK). Samples were prepared by depositing 0.3 μL of matrix (2,5-dihydroxybenzoic acid in methanol) onto the stainless steel slide followed by 0.3-μL aliquot of the analyte. Analyte ions were desorbed from the matrix with a 337-nm nitrogen laser irradiation. TOF spectra were acquired in a reflectron high voltage mode using 20-kV extraction voltage. Each spectrum was an average of 50 shots.

Results and Discussion

Recent advances in mass spectrometry, such as introduction of the electrospray ionization (ESI) technique, allow direct studies of biologically relevant noncovalent complexes to be carried in the gas phase [12]. One of these studies, which is of particular relevance to the topic of the present work, focused on the observation of ferric ion complexation with a synthetic analog of a bacterial siderophore, ligand L [13]. It must be noted that the vast majority of noncovalent complexes, including metal ion-ligand systems, can survive a transition from solution to gas phase only under mild conditions of electrospray [12]. The attempts to detect complexation of Fe^{3+} and Co^{3+} ions by phytosiderophores under harsh conditions of FAB [8] have failed due to prompt reduction of these ions to Fe^{2+} and Co^{2+}, correspondingly. Another group of siderophores, exochelins from *M. tuberculosis*, have been recently studied by a combination of LSIMS and electrospray ionization mass spectrometry [14]. While only intact ferri-exochelin cations have been detected by ESI mass spectrometry, the LSIMS spectra contained numerous cationic species, including chelates of Na, Mg^{II}, Al^{III}, Fe^{III}, as well as uncomplexed analyte cations [14].

The LSIMS spectrum of the iron-free ferrichrome is presented on Figure 2a. The most abundant peak at m/z 688.2 corresponds to a protonated peptide ion $[M + H]^+$. The intact ferrichrome molecule does not carry a net electrical charge at neutral pH, because the positive charge of Fe^{III} is compensated by a net negative charge of the oxygen atoms of the cyclic peptide (M) modified ornithine side chains, the monoisotopic molecular weight of this neutral intact species $[M\text{-}3H + Fe^{III}]^0$ being 740.2 amu. To be detected with a mass spectrometer, this complex must be protonated or canonized by an alkali metal ion. Figure 2b shows the positive ion LSIMS spectrum of ferrichrome. The most abundant ions correspond to $[M\text{-}2H + Fe^{III}]^+$ (at m/z 741.0) and $[M\text{-}3H + Fe^{III} + Na]^+$ (at m/z 763.0). Interestingly, no

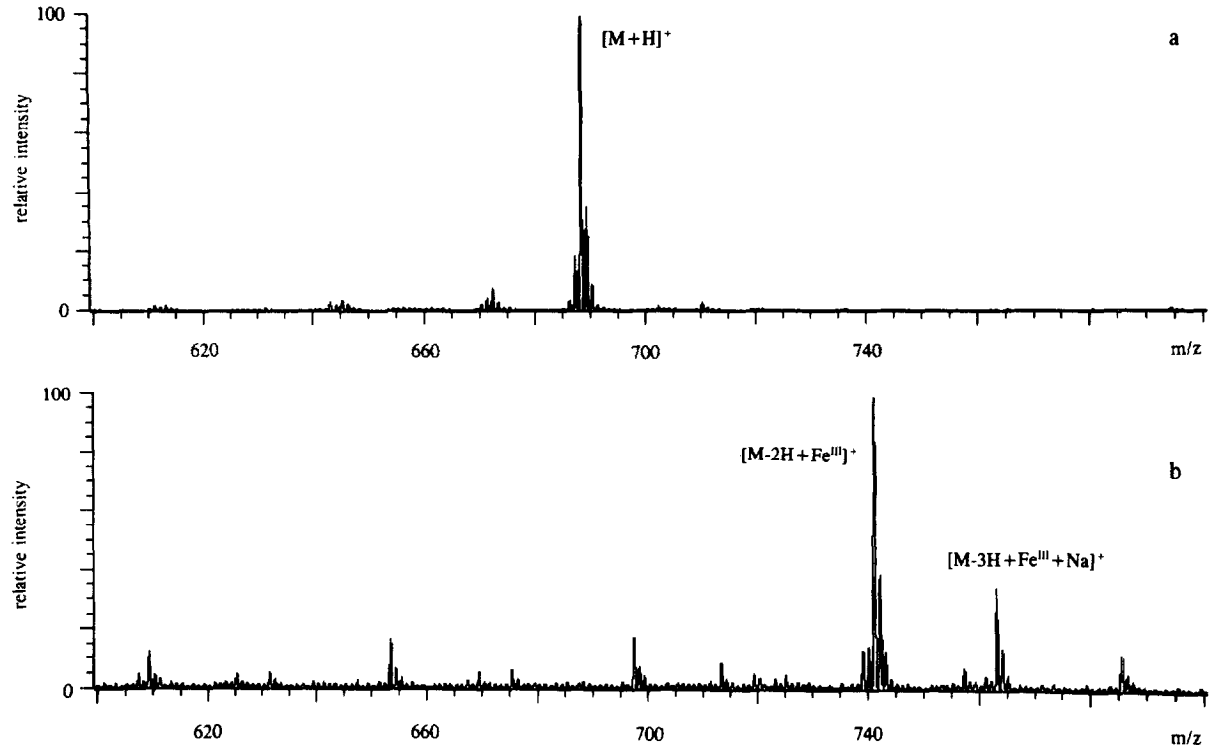

Figure 2. Positive ion LSIMS spectra of ferrichrome: (**a**) iron-free peptide and (**b**) HPLC-purified complex.

signal corresponding to either protonated ($[M + H]^+$ at m/z 688.3) or sodiated ($[M + Na]^+$ at m/z 710.3) peptide lacking ferric ion has been observed, nor could be detected any ionic signal corresponding to iron (Fe^{n+}, n = 1–3) escaping its carrier.

To study the chelation and solubilization of ferric ions by molecules of the iron-free ferrichrome, ferric citrate was added to a 1-mg/mL solution of the siderophore (in 50% methanol). No color change of the solution was visible following precipitation of the salt. The positive ion LSIMS spectrum of the supernatant of the suspension was recorded immediately following the addition of ferric citrate. No signal of a Fe^{III}-peptide complex was detected at that time; the spectrum appeared to be an exact replica of that presented in Figure 2a. The peptide-ferric citrate mixture was then sonicated in an ultrasonic bath at room temperature, and aliquots of the supernatant were analyzed following 10-min, 30-min, and 1-h time intervals. The resultant mass spectra (Figure 3) show consistent increase of the content of the metal ion-cyclic peptide complex; the ionic signal of the uncomplexed peptide, $[M + H]^+$, is not present in the final spectrum (Figure 3c).

To compare complexation of Fe^{III} by ferrichrome with other metals, excess calcium acetate and zinc acetate were added to solutions of the iron-free ferrichrome in quantities enough to saturate the solutions with the salts. Both mixtures were mass analyzed following a 30-min sonication period (Figure 4). The peptide has been found to chelate Ca^{2+} ions, as reflected by the appearance of abundant $[M\text{-}H + Ca^{II}]^+$ and $[M\text{-}3H + 2Ca^{II}]^+$ ions in the spectrum. However, metal-free peptide cation $[M + H]^+$ is always present in the spectrum, suggesting that Ca^{II} affinity of ferrichrome is lower compared to its Fe^{III} affinity. Almost no ions corresponding to Zn^{II} adducts can be observed in the spectrum of the iron-free ferrichrome/zinc acetate mixture (Figure 4b). The striking difference in the complexation behavior of Ca^{II} and Zn^{II} probably reflects the fact that the Zn^{2+} ion is a soft acid (unlike Ca^{2+} and Fe^{3+}), and therefore binds much weaker to oxamide (which is a hard base).

Further insight on the structure of ferrichrome ions and their relevance to the structure of intact metal-ligand complex can be provided by methods of tandem mass spectrometry. Collision-induced dissociation of specific peptide-metal ion complexes has shown a promise of being able to provide valuable information on the location of the chelation sites [15]. In the present work, both intact and iron-free ferrichrome cations, $[M\text{-}2H + Fe^{III}]^+$ and $[M + H]^+$ have been subjected to high-energy CID. The most abundant high-mass fragment ions in the spectrum of the dissociation of the iron-free ferrichrome cation (Figure 5a) are those due to the loss of H_2O, $(OC)CH_2$, and CO. The latter one is a typical "ring-opening" fragment, which is characteristic for all cyclic peptides [16]. The loss of $(OC)CH_2$ may also result from a ring-opening process [16], as well as from the cleavage of labile amide bond at the side chains of modified ornithine residues. Most other peaks

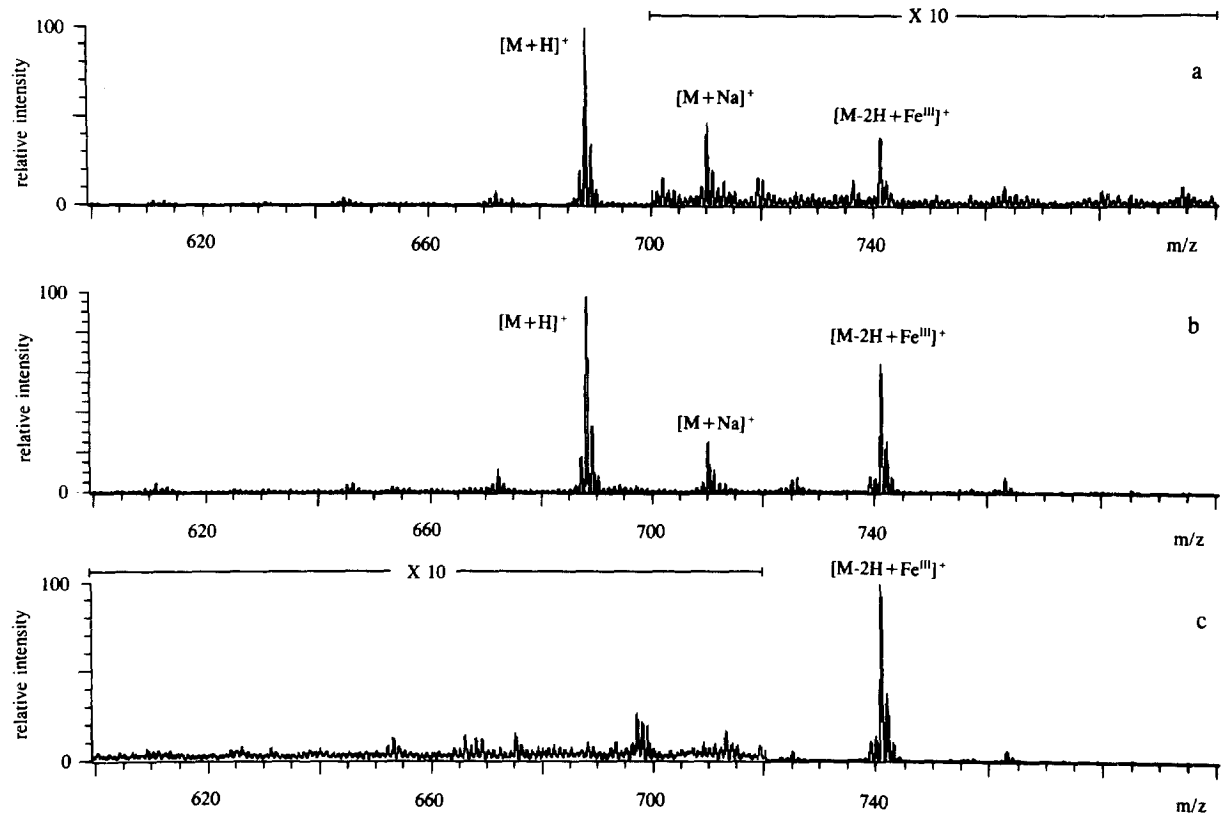

Figure 3. Solubilization of iron by ferrichrome: positive ion LSIMS spectra of iron-free ferrichrome sonicated with an excess of ferric citrate for (**a**) 10 min, (**b**) 30 min and (**c**) 1 h.

in the spectrum correspond to ring-opening processes resulting from elimination of one or more amino acid residues.

Not surprisingly, all fragments of the intact ferrichrome cation, $[M\text{-}2H + Fe^{III}]^+$, observed in the CID spectrum (Figure 5b), contain ferric ion (all others are very unlikely to be detected, since a departure of Fe^{III} from a singly charged precursor ion would most likely change the polarity of the resulting fragment). To simplify the interpretation of both CID spectra we have shifted the mass-to-charge ratio scale of the intact ferrichrome cation CID spectrum (Figure 5b) to higher masses by 53 amu ($^{56}Fe\text{-}3^1H$). The dotted lines on Figure 5 show the pairs of matching peaks, M_{fr}^+ and $[M_{fr}\text{-}3H + Fe^{III}]^+$, corresponding to analogous fragment ions present in both spectra. Our attention, however, has been directed mostly towards the "unmatched" fragment ion peaks, because those may provide information on how the fragmentation of the cyclic peptide is affected by the presence of Fe^{III}. This information can be used to determine the location of the ferric ion chelation sites within the siderophore unaffected by the solvent.

The most noticeable difference between the two CID spectra is the absence of the fragment ions due to the loss of ketene moiety $CH_2(CO)$ in the CID spectrum of the intact ferrichrome cation (Figure 5b). This fact may be rationalized by assuming that the major process leading to the loss of ketene in the iron-free ferrichrome cations is a cleavage of a labile hydroxamide bond. This dissociation process may have a significantly lower rate constant for the metal ion-peptide complex if the hydroxamate groups of the peptide become involved in ligation of the ferric ion.

Both CID spectra on Figure 5 contain fragment ion peaks associated with ring-opening processes resulting in losses of one or more glycine or ornithine amino acid residues. However, the fragment ions resulting from the loss of the two ornithine residues from a metal-containing cation, $[OrnGly_3\text{-}H_2O\text{-}2H + Fe^{III}]^+$ or $[OrnGly_3\text{-}H_2O\text{-}H + Fe^{III}]^{2+}$, were not detected among the CID products of $[M\text{-}2H + Fe^{III}]^+$ (Figure 5b), whereas a prominent fragment ion peak $[OrnGly_3\text{-}H_2O + H]^+$ is present in the CID spectrum of the iron-free peptide cation (Figure 5a). This indicates the inability of a single hydroxamate to coordinate Fe^{III} effectively. Interestingly, very prominent fragment ions resulting from the loss of one ornithine residue are present in CID spectra of both intact and iron-free ferrichrome cation. This suggests that a minimal amount of two hydroxamates is required to maintain a stable Fe^{III} coordination complex in the gas phase. Abundant fragment ions resulting from the consecutive elimination of all glycine residues are also present in both CID spectra, suggesting that heteroatoms of the peptide backbone do not play any significant role in the complexation of the ferric ion.

In the negative ion mode, a reduction of Fe^{III} to Fe^{II}

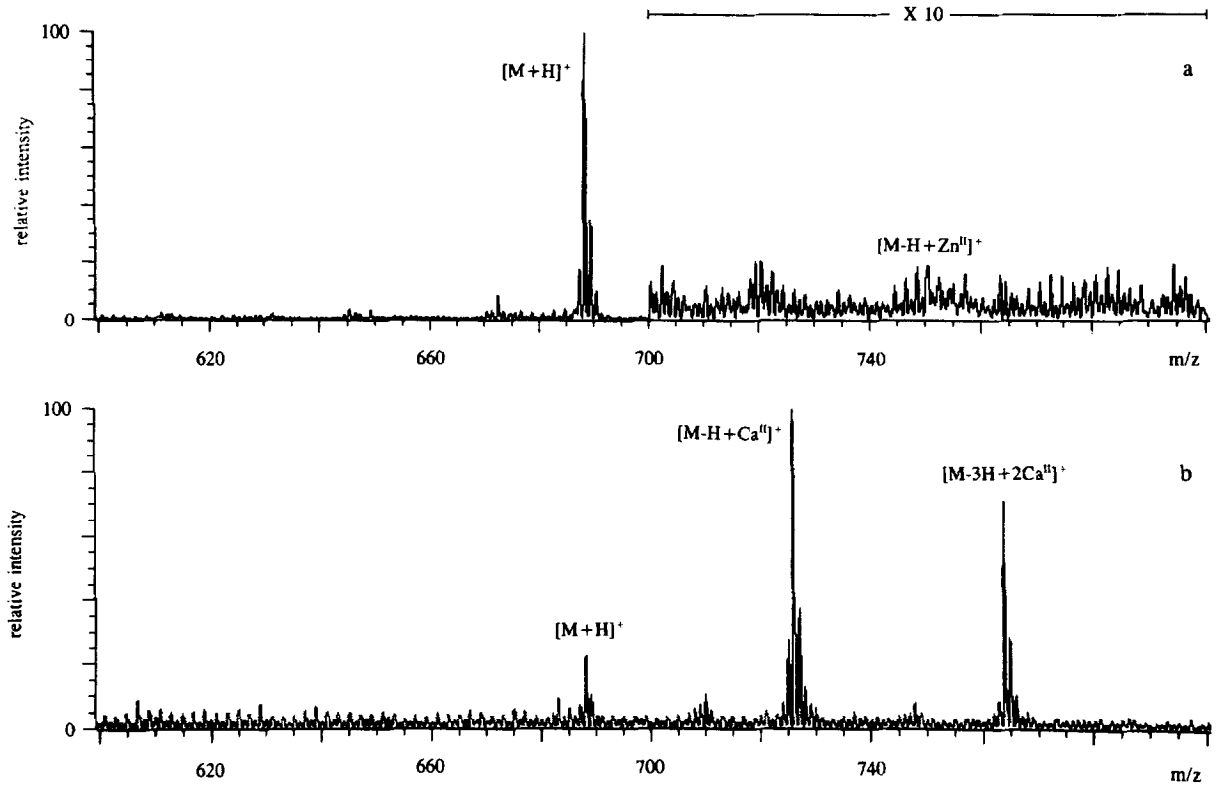

Figure 4. Complexation of Zn^{II} and Ca^{II} by ferrichrome: positive ion LSIMS spectra of iron-free ferrichrome incubated with (**a**) zinc acetate and (**b**) calcium acetate.

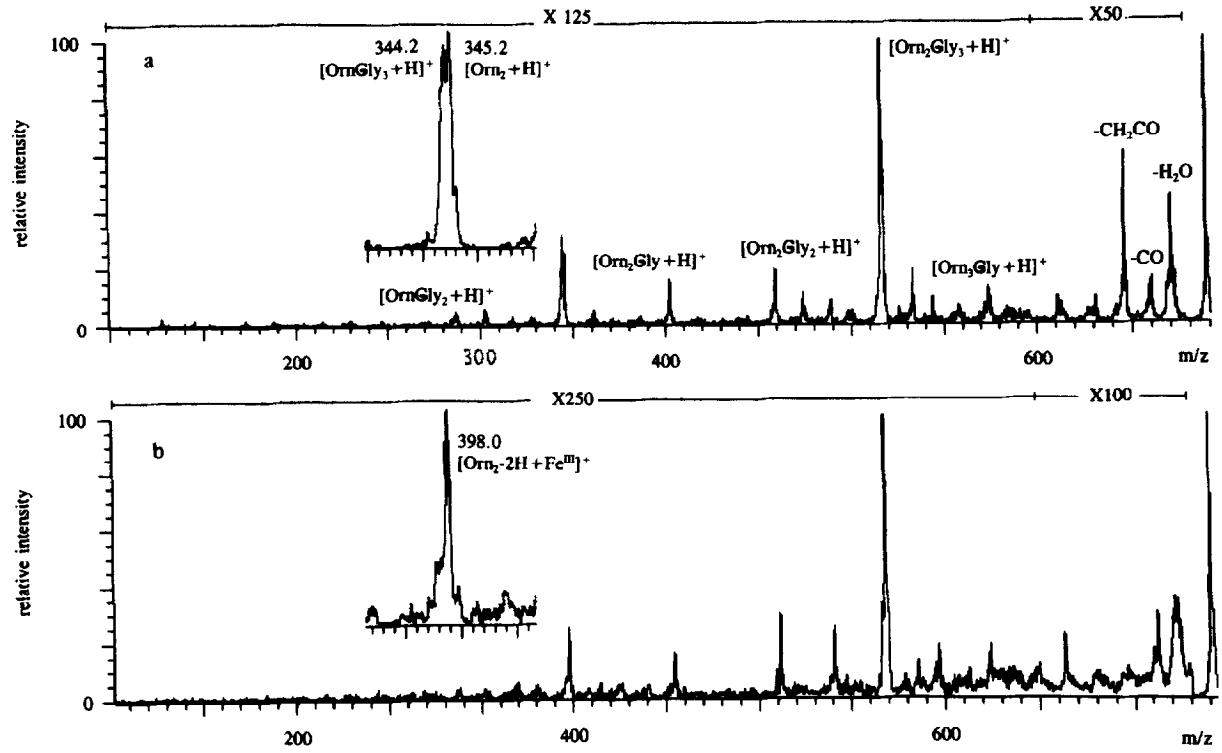

Figure 5. High-energy CID fragment ion spectra of a protonated iron-free ferrichrome cation $[M + H]^+$ at m/z 688.2 (**a**) and a metal ion-peptide cationic complex $[M\text{-}2H + Fe^{III}]^+$ at m/z 741.0 (**b**).

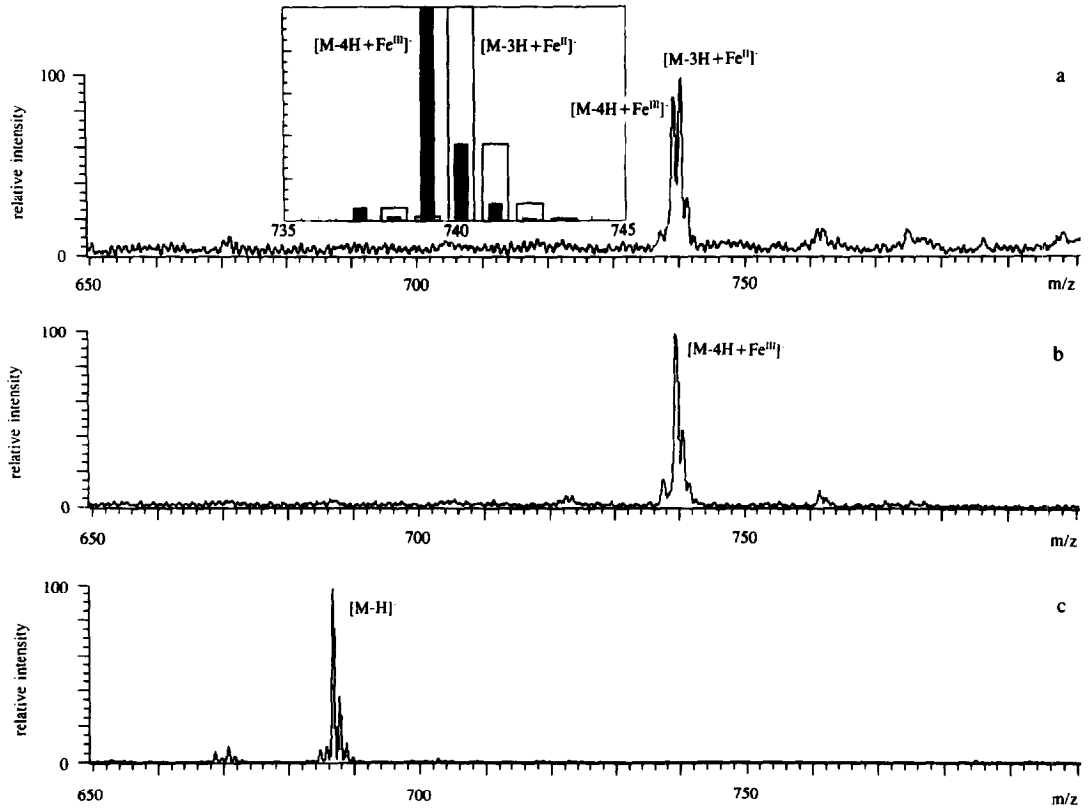

Figure 6. Negative ion LSIMS spectra of ferrichrome: HPLC-purified metal ion-peptide complex using (**a**) 3-NBA and (**b**) MTG as matrices, and (**c**) an iron-free peptide using MTG as a matrix. Inserts: calculated isotopic distributions for ferrichrome anions containing Fe^{III} and Fe^{II}.

was expected to take place. Indeed, when 3-NBA was employed as a matrix, a mixture of the two oxidation states has been detected, corresponding anions being separated by 1 amu (Figure 6a). These correspond to $[M\text{-}4H + Fe^{III}]^-$ (calculated molecular weight 739.2 amu, measured 739.3 amu) and $[M\text{-}3H + Fe^{II}]^-$ (calculated molecular weight 740.2 amu, measured 740.3 amu) anions. Interestingly, the reduction does not take place when another matrix, MTG, is used to desorb ferrichrome anions: the measured isotopic distribution for the most prominent peak in the spectrum is very close to calculated natural isotopic distribution for the Fe^{III}-containing anion (Figure 6b). The most likely reason for the different redox behavior of the two matrices is the fact that under LSIMS conditions MTG tends to form an even-electron (deprotonated) anion, while 3-NBA forms predominantly an odd-electron anion (radical ion), which may promote reduction of the peptide-bound ferric ion:

$$NBA^{\cdot -} + [M\text{-}3H + Fe^{III}]^0 \rightleftarrows NBA^0 + [M\text{-}3H + Fe^{II}]^-$$

The enzymatic reduction of the ferric ion to ferrous ion within a hydroxamate-based siderophore is a precursor to an intracellular release of iron [4]. However, our data indicate that reduction of Fe^{III} to Fe^{II} does not lead to a prompt dissociation of the metal ion from the peptide: the iron-free anions of ferrichrome, $[M\text{-}H]^-$, have not been detected in any of the negative ion LSIMS spectra of the high-performance liquid chromatography (HPLC)-purified ferrichrome, even in the presence of a strong ionic signal of a peptide-ferrous ion complex (Figure 6a). It is possible that other factors (such as the solution pH) may contribute to the surprising stability of this partially reduced metal ion-peptide complex.

High-energy CID spectra of both iron-free and Fe^{III}-containing ferrichrome anions have been also acquired on a sector instrument (Figure 7). The striking difference between the two spectra provides additional information on the location of the ferric ion within the peptide. First, the most abundant fragment ion in the CID spectrum of $[M\text{-}H]^-$ is due to the loss of water, i.e., $[M\text{-}H_2O\text{-}H]^-$, whereas the most prominent peak in the CID spectrum of an intact ferrichrome anion, $[M\text{-}4H + Fe^{III}]^-$, results from the loss of ammonia, i.e., $[M\text{-}NH_3\text{-}4H + Fe^{III}]^-$. The loss of ketene gives rise to a prominent peak in the CID spectrum of the iron-free ferrichrome anion, while the relative intensity of the analogous peak in the CID spectrum of the intact ferrichrome is significantly lower.

The only prominent peak present in both spectra, that is associated with the loss of an amino acid residue, results from elimination of two glycine residues. None of the fragments, resulting from elimination of one or

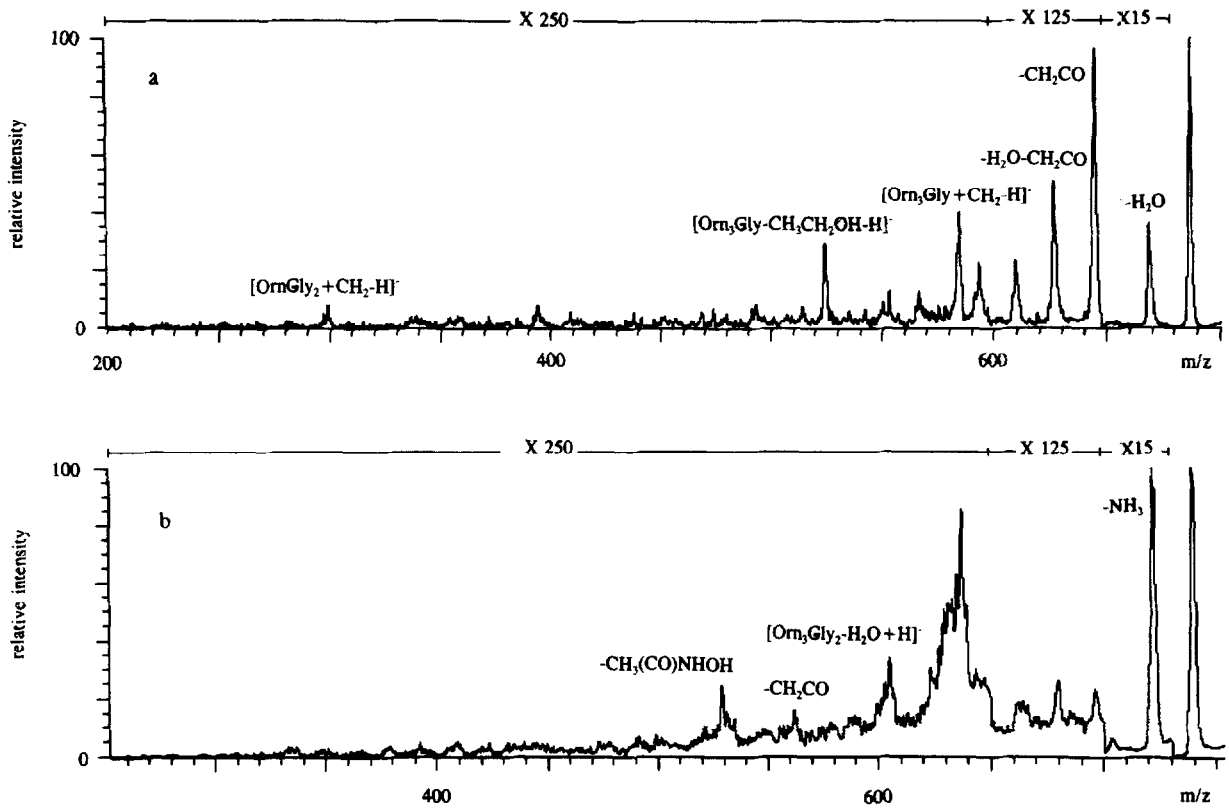

Figure 7. High-energy CID fragment ion spectra of deprotonated iron-free ferrichrome anion $[M-H]^-$ at m/z 686.3 (**a**) and a metal ion-peptide anionic complex $[M-4H + Fe^{III}]^-$ at m/z 739.1 (**b**).

more ornithine residues, is present in the CID spectrum of the intact ferrichrome anion (Figure 7b). Another interesting feature of this spectrum is the presence of a series of fragment ion peaks that appear to be derivatives of the $[Orn_3Gly + CH_2\text{-}4H + Fe^{III}]^-$ fragment ion and result from consecutive losses of water (at m/z 606), ketene (m/z 562), and methanol (at m/z 529) molecules. All three of these peaks lack ferric ion (the excess of the negative charge is probably compensated by the intramolecular proton transfers during dissociation). These observations provide further reinforcement to the conclusion that hydroxamate oxygen atoms play an important role in stabilizing the ferric ion within the peptide, and that the metal ion chelation cannot be carried effectively by the heteroatoms of the peptide backbone.

Ferrichrome has been also subjected to the mass spectral analysis using matrix-assisted laser desorption ionization (MALDI) in this work. MALDI is only rarely used to study specific noncovalent interactions of biomolecules [17] primarily due to extreme pK_A values of most UV matrices employed to facilitate ion desorption. Nevertheless, because the typical MALDI conditions are generally considered to be rather "soft," compared to that of LSIMS, we have expected the metal ion-peptide complex to survive desorption by MALDI. It came as a surprise to us that the intact ferrichrome appeared to be rather fragile under conditions of MALDI. Although protonated ferrichrome $[M\text{-}2H + Fe^{III}]^+$ is present in the positive ion MALDI spectra, its intensity is significantly lower compared to that of the analyte ions lacking Fe^{III}, $[M + Na]^+$ in particular (Figure 8a). It must be noted that the ion intensity ratio $[M\text{-}2H + Fe^{III}]^+/[M + Na]^+$ increases when the laser irradiation power is lowered. In fact, $[M\text{-}2H + Fe^{III}]^+$ was determined to be a predominant high-mass ion in the linear mode experiments, which are performed at much lower laser output, as compared to the reflectron mode (data not shown). The three most abundant ion peaks in the low-mass region of the spectrum (Figure 8a) are those of Na^+, Fe^{2+}, and K^+. Sodium and potassium cations are ubiquitous contaminants and are usually prominent in all MALDI spectra. Abundances of other metal anions in MALDI spectra are usually at least an order of magnitude lower that of Na^+ and K^+. In our case, the signal intensity of the Fe^{2+} peak is close to that of Na^+ and exceeds K^+. Therefore, it seems to be very likely that the observed anomalously high ionic signal of Fe^{2+} could be a result of dissociation of a reduced, Fe^{II}-containing ferrichrome cation. This assumption is further supported by the fact that no Fe^{3+} ionic signal has been detected.

The anions of the intact ferrichrome are missing in the negative ion MALDI spectrum altogether (Figure 8b), the most prominent high-mass ion being $[M-H]^-$. It appears that acidic matrices used in MALDI facilitate the reduction process of Fe^{III} to Fe^{II} and/or catalyze

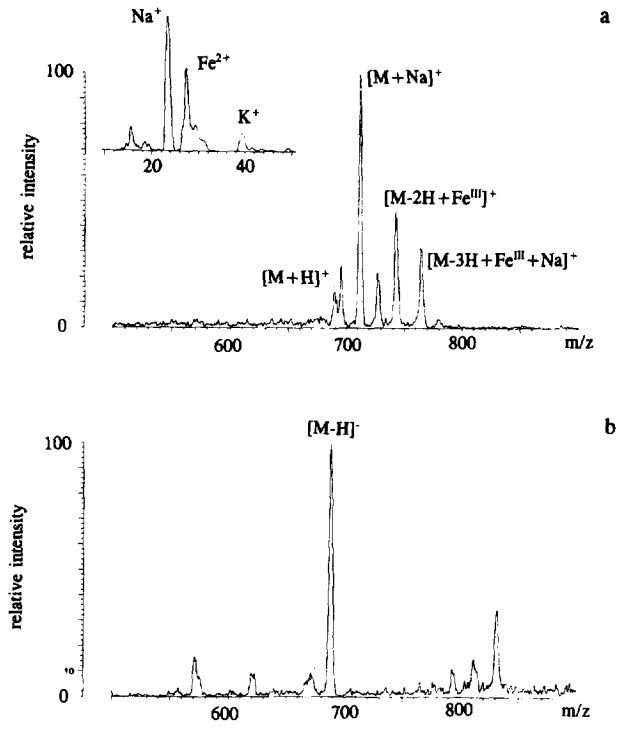

Figure 8. (a) Positive and (b) negative ion MALDI mass spectra of HPLC-purified ferrichrome.

dissociation of iron from ferrichrome (e.g., by protonating the negatively charged hydroxamate groups).

Conclusions

Ferrichrome, a complex of a cyclic peptide and Fe^{III}, appears to be remarkably stable under conditions of LSIMS. Reduction of ferric ion to ferrous ion within the metal-peptide complex does not necessarily result in dissociation of the complex. The stability of the metal ion-peptide complex is significantly lower under typical MALDI conditions, presumably due to the influence of acidic matrices. The appearance of high-energy CID spectra of ferrichrome cation, generated by LSIMS, suggests that Fe^{III} is still coordinated by hydroxamate oxygen atoms of the ornithine side chains in the gas phase, just as in solution or crystal. A minimum of four oxygen atoms is required to chelate the ferric ion. This chelation is rather specific, as heteroatoms of the peptide backbone do not appear to be able to coordinate effectively the metal ion when the number of available hydroxamate oxygen donors is reduced by fragmenting the peptide.

Acknowledgment

This work was supported in part by the National Institutes of Health grant no. RO1GM33967.

References

1. Neilands, J. B.; Konopka, K.; Schwyn, B.; Coy, M.; Francis, R. T.; Paw, B. H.; Bagg, A. In *Iron Transport in Microbes, Plants and Animals*; Winkelmann, G.; Van der Helm, D.; Neilands, J. B., Eds.; VCH: New York, 1987; pp 3–33.
2. Beveridge, T. J. In *Metal Ions and Bacteria*; Beveridge, T. J.; Doyle, R. J., Eds.; Wiley: New York, 1989; pp 1–29.
3. Neilands, J. B. *J. Biol. Chem.* **1995,** *270,* 26723–26726.
4. Raymond, K. N.; Carrano, C. J. *Acc. Chem. Res.* **1979,** *12,* 183–190.
5. Miller, M. J.; Malouin, F. In *The Development of Iron Chelators for Clinical Use*; Bergeron, R. J.; Brittenham, G.M., Eds.; CRC: Boca Raton, FL, 1994; pp 275–306.
6. Van der Helm, D.; Jalal, M. A. F.; Hossain, M. B. In *Iron Transport in Microbes, Plants and Animals*; Winkelmann, G.; van der Helm, D.; Neilands, J. B., Eds.; VCH: New York, 1987; pp 135–165.
7. Matzanke, B. F. In *Iron Transport in Microbes, Plants and Animals*; Winkelmann, G.; van der Helm, D.; Neilands, J. B., Eds.; VCH: New York, 1987; pp 251–284.
8. (a) Kenny, P. T. M.; Nomoto, K. *Analyst* **1994,** *119,* 891–895; (b) Kenny, P. T. M.; Nomoto, K. *J. Mass Spectrom. Rapid Commun. Mass Spectrom.* **1995,** S13–S18.
9. Neilands, J. B. *J. Am. Chem. Soc.* **1952,** *74,* 4846–4847.
10. Cooper, S. R.; McArdle, J. V.; Raymond, K. N. *Proc. Natl. Acad. Sci. USA* **1978,** *75,* 3551–3554.
11. (a) Wayne, L. N.; Nielands, J. B. *J. Bacteriol.* **1975,** *121,* 497–503; (b) Feinstone, W. H., unpublished.
12. (a) Loo, J. A. *Bioconjugate Chem.* **1995,** *6,* 644–665; (b) Przybylski, M.; Glocker, M. O. *Angew. Chem. Int. Ed. Engl.* **1996,** *35,* 806–826.
13. Jaquinod, M.; Leize, E.; Potier, N.; Albrecht, A.-M.; Shanzer, A.; Van Dorsselaer, A. *Tetrahedron Lett.* **1993,** *34,* 2771–2774.
14. Gobin, J.; Moore, C. H.; Reeve, J. R.; Wong, D. K.; Gibson, B. W.; Horwitz, M. A. *Proc. Natl. Acad. Sci. USA* **1995,** *92,* 5189–5193.
15. (a) Hu, P.; Gross, M. L. *J. Am. Chem. Soc.* **1993,** *115,* 8821–8828; (b) Zhao, H.; Reiter, A.; Teesch, L. M.; Adams, J. *J. Am. Chem. Soc.* **1993,** *115,* 2854–2863; (c) Loo, J. A.; Hu, P.; Smith, R. D. *J. Am. Soc. Mass Spectrom.* **1994,** *5,* 959–965; (d) Hu, P.; Loo, J. *J. Am. Chem. Soc.* **1995,** *117,* 11314–11319; (e) Hu, P.; Sorensen, C.; Gross, M. L. *J. Am. Soc. Mass Spectrom.* **1995,** *6,* 1079–1085; (f) Gatlin, C. L.; Rao, R. D.; Tureček, F.; Vaisar, T. *Anal. Chem.* **1996,** *68,* 263–270; (g) Nemirovski, O. V.; Gross, M. L. *J. Am. Soc. Mass Spectrom.* **1996,** *7,* 977–980.
16. Eckart, K. *Mass Spectrom. Rev.* **1994,** *13,* 23–55.
17. (a) Woods, A. S.; Buchsbaum, J. C.; Worral, T. A.; Berg, J. M.; Cotter, R. J. *Anal. Chem.* **1995,** *67,* 4462–4465; (b) Cohen, L. R. H.; Strupat, K.; Hillenkamp, F. *Proceedings of the 44th ASMS Conference on Mass Spectrometry and Allied Topics*; Portland, OR, 1996; p 1049; (c) Glocker, M. O.; Bauer, S. H. J.; Kast, J.; Volz, J.; Przybylski, M. *J. Mass Spectrom.* **1996,** *31,* 1221–1227.